EFFECTS OF LASER RADIATION AND NANO – POROUS LINING ON THE RAYLEIGH – TAYLOR INSTABILITY IN AN ABLATIVELY LASER ACCELERATED PLASMA.

N. Rudraiah

National Research Institute for Applied Mathematics (NRIAM),
492/G, 7th Cross, 7th Block (west), Jayanagar,
Bangalore – 560 082.
And
UGC-CAS in Fluid Mechanics, Department of Mathematics
Bangalore University, Bangalore-560 001.

1. INTRODUCTION

For efficient extraction of Inertial Fusion Energy (IFE) it is essential to reduce the growth rate of surface instabilities in laser accelerated ablative surface of IFE target. The following three different types of surface instabilities are observed :

- Rayleigh – Taylor Instability (RTI)
- Kelvin – Helmholtz Instability (KHI)
- Richtmyer – Meshkov Instability (RMI)

At present the following mechanisms are used to reduce the RTI growth rate.

- Gradual variation of density assuming plasma as incompressible heterogeneous fluid without surface tension.
- Assuming plasma as compressible fluid without surface tension.
- IFE target shell with foam layer.

Numerous numerical and experimental data for RTI growth rate at the ablation surface for compressible fluid fits.

$$n = A\sqrt{\frac{\ell g}{1+\varepsilon\,\ell L}} - \beta\,\ell\, v_a \qquad \textbf{(1.1)}$$

Rudraiah (2003) derived an analytical expression

$$n = \frac{1}{3}\ell^2\left[1-\left(\frac{\ell^2}{B}\right)\right] - \beta\,\ell\, v_a \qquad \textbf{(1.2)}$$

for a target lined with porous layer comprising nanotube, considering viscous incompressible fluid. Here $\mathrm{B} = \delta h^2 / \gamma$ is the Bond number, γ is the surface tension, $\delta = g\left(\rho_p - \rho_f\right)$, $\beta = \frac{3\alpha\sigma}{4+\alpha\sigma}$, $\mathrm{v}_a = \frac{\left(4+\alpha\sigma\right)}{12\left(1+\alpha\sigma\right)}\ell\left(1-\frac{\ell^2}{\mathrm{B}}\right)$, ρ_p and ρ_f are the density of porous lining and fluid respectively. Density in the range 5< ρ_p <103 kg/cm^{3,} $k = \left(1.1 - 2.7\right)\times 10^{-5}\ in^2$ for foam metal and $k \approx \left(1.0 - 2.48\right)\times 10^{-6}\ in^2$ for aloxite metal and ε = (0.016 – 0.027)

Choosing suitable values for the constants A, ε and β one can fit the available data.

Authors	*A*	ε	β	n_m
Takabe *et al* (1985)	0.90	0.0	3.00	0.45 n_{bn}
Lindl *et al* (1995)	1.00	1.0	3.00	
Betti *et al* (1995)	0.98	1.0	1.70	
Kilkenny *et al* (1994)	0.90	1.0	3.00	
Knauer *et al* (2000)	0.90	1.0	3.02	
Rudraiah (2003)	1.00	1.0	0.75 2.86	0.79 n_{bm} (α =0.1, σ = 4) *0.26* n_{bm} (α =4, σ = 20)

2. MATHEMATICAL FORMULATION.

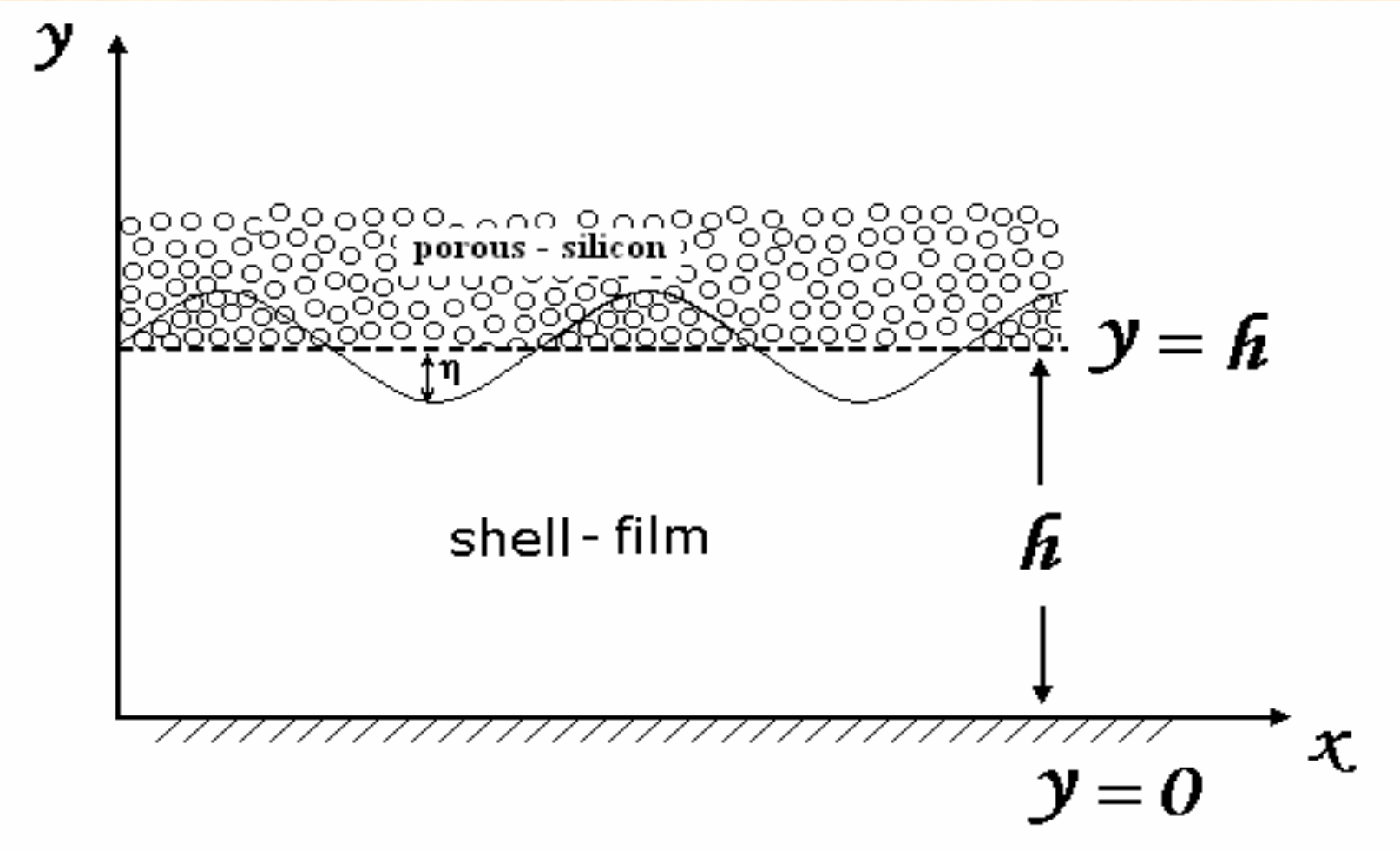

Fig 1. Physical Configuration

The conservation of momentum:

$$\overline{\rho}\left(\frac{\partial \vec{q}}{\partial t}+\left(\vec{q}\cdot\nabla\right)\vec{q}\right)=-\nabla p+\overline{\mu}_f\nabla^2\vec{q}-K\vec{q}+\overline{\mu}_h\vec{J}\times\vec{H} \qquad \textbf{(2.1)}$$

The conservation of mass for compressible Boussinesq fluid

$$\nabla\cdot\vec{q}=0 \qquad \textbf{(2.2)}$$

$$\overline{\rho}=\rho_o\left[1-\alpha_T\left\{X_p\left(T_p-T_f\right)+T_f-T_o\right\}\right]$$

The conservation of energy

$$\left(X_p\left(M-1\right)+1\right)\frac{\partial T}{\partial t}+\left(\vec{q}\cdot\nabla\right)T=\left(X_p\left(\kappa'-1\right)+1\right)\nabla^2T-\hat{n}\cdot\nabla I \qquad \textbf{(2.3)}$$

where $\vec{J} = \overline{\sigma}_h \left[\vec{E} + \overline{\mu}_h \vec{q} \times \vec{H} \right]$ =Current density,

$$\nabla \cdot \vec{H} = 0, \quad \nabla \times \vec{E} = -\frac{\partial \vec{H}}{\partial t}, \quad \nabla \cdot \vec{E} = 0$$

$\overline{\rho} = \rho_f \left[1 + X_p \left(\frac{\rho_p}{\rho_f} - 1 \right) \right]$ = Density,

$\overline{\mu} = \mu_f \left[1 + X_p \left(\frac{\mu_{ef}}{\mu_f} - 1 \right) \right]$ = Viscosity,

$\overline{\mu}_h = \mu_h \left[1 + X_p \left(\frac{\mu_p}{\mu_h} - 1 \right) \right]$ = Magnetic permeability

$\overline{\sigma}_h = \sigma_h \left[1 + X_p \left(\frac{\sigma_{hp}}{\sigma_h} - 1 \right) \right]$ = Electrical conductivity

$$K = X_p\left(\frac{\mu_f}{k} + \frac{\rho_p C_b}{\sqrt{k}}|q|\right) \qquad \kappa' = \frac{\kappa_{ef}}{\kappa} \qquad m = \frac{\left(\rho C_p\right)^*}{\left(\rho C_p\right)_f}$$

$$\left(\rho C_p\right)^* = \varepsilon\left(\rho C_p\right)_f + (1-\varepsilon)\left(\rho C_p\right)_s$$

$$X_p = \begin{cases} 0 & \text{for shell} \\ 1 & \text{for porous lining.} \end{cases}$$

Boundary Conditions

$$u = v = 0 \quad at \quad y = 0 \quad and \quad \frac{du}{dy} = -\alpha\sigma u \quad at \quad y = 1$$

3. DISPERSION RELATION WITH LASER RADIATION

In this section we derive the dispersion relation as well as the temperature distribution incorporating the laser radiation effect.

3.1 Dispersion relation

$$u = \frac{\{Mch[M(1-y)] + \alpha\sigma Sh[M(1-y)] + \alpha\sigma[Sh(My) - Sh(M)] - Mch(M)\}}{[Mch(M) + \alpha\sigma Sh(M)]} \times \frac{P}{M^2} \quad \textbf{(3.1)}$$

where $M = \mu H_o h \sqrt{\frac{\sigma_h}{\mu_f}}$ is the Hartman number; $\sigma = \frac{h}{\sqrt{k}}$ is the porous parameter; Cosh (θ) *and Sinh* (θ) are denoted by *Ch* (θ) and Sh (θ) *respectively.*

$$v(1) = \left\{ \frac{2\alpha\sigma[1 - Ch(M)] + (\alpha\sigma - 1)MSh(M) + M^2 Ch(M)}{M^3[MCh(M) + \alpha\sigma Sh(M)]} \right\} \frac{\partial^2 p}{\partial x^2} \quad \textbf{(3.2)}$$

$$n = n_b - \beta \ell v_a \quad \textbf{(3.3)}$$

where *n* is the growth rate, ℓ is the wave number,

$$\beta = \frac{M^3 - 3(M - th\,M) + \alpha\sigma(M^2 - 3)\,th\,M + \dfrac{6\alpha\sigma(ch\,M - 1)}{M\,ch M}}{3\left[M - th\,M + \alpha\sigma\,th\,M + \dfrac{2\alpha\sigma(1 - ch\,M)}{M\,ch\,M}\right]} \qquad \textbf{(3.4)}$$

a constant, v_a is the velocity of flow across the ablative front given by

$$v_a = \frac{M - th\,M + \alpha\sigma\,th\,M + \dfrac{2\alpha\sigma(1 - ch\,M)}{M\,ch\,M}}{M^3\left(1 + \alpha\sigma\dfrac{th\,M}{M}\right)}\,\ell\left(\delta - \frac{\ell^2}{B}\right) \qquad \textbf{(3.5)}$$

$B = \delta_o h^2 / \gamma$ is the Bond number, $\delta = 1$ or $\left(\theta_{p_1} - \theta_{f_1}\right)$

where suffix 1 denotes the values of θ at y =1, *and*

$$n_b = \frac{\ell^2}{3}\left(\delta - \frac{\ell^2}{B}\right) \qquad \textbf{(3.6)}$$

when M $\rightarrow$ 0, Eq. (3.3) reduces to Rudraiah (2003)

$$n_1 = n_b - \beta_1 \, \ell \, v_{a_1} \qquad \textbf{(3.7)}$$

where

$$\beta_1 = \frac{3\,\alpha\,\sigma}{4+\alpha\,\sigma} \qquad \textbf{(3.8)} \qquad v_{a_1} = \frac{4+\alpha\,\sigma}{12\,(1+\alpha\,\sigma)}\,\ell\left(\delta - \frac{\ell^2}{B}\right) \qquad \textbf{(3.9)}$$

In the absence of nanostructure porous lining, (*k* i.e., $\sigma \rightarrow 0$) the growth rate (3.3) tends to

$$n_2 = n_b - \beta_2 \, \ell \, v_{a2} \qquad \textbf{(3.10)}$$

where

$$\beta_2 = \frac{M^3 - 3\,(M - th\,M)}{3\,(M - th\,M)} \qquad \textbf{(3.11)} \qquad v_{a_2} = \frac{M - th\,M}{M^3} \qquad \textbf{(3.12)}$$

In the case of using Eq. (3.9) which is $(n_b)_p$; we have

$$n_3 = (n_b)_p - \beta_3 \, \ell \, v_{a_3}$$

$$\beta_3 = \frac{M^3 - 3\,(M - thM) + \alpha\sigma(M^2 - 3)\,thM + \dfrac{6\alpha\sigma(chM - 1)}{M\,chM} - 3\alpha\sigma M^2\left(1 + \alpha\sigma\, thM\right)}{3\left[M - thM + \alpha\,\sigma\, thM + \dfrac{2\,\alpha\,\sigma\,(1 - chM)}{M\,chM}\right]}$$

v_{a_3} is the same as Eq. (3.5)

3.2 Temperature distribution

For the shell – film $$\mathrm{v}_a \frac{\partial T_f}{\partial y} = \kappa_f \frac{\partial^2 T_f}{\partial y^2} + I_o\,\Omega\, e^{-\Omega y} \qquad \textbf{(3.13)}$$

For the porous – silicon layer $$0 = \kappa_p \frac{\partial^2 T_p}{\partial y^2} \pm I_o\,\Omega\, e^{-\Omega y} \qquad \textbf{(3.14)}$$

where κ_f and κ_p are the thermal diffusivity for shell – film and porous – silicon lining. The selection of a particular sign in Eq. (3.14) will depend on the physical situation. If we choose positive sign, then θ_p will be negative implying energy will be lost. The problem considered in this paper requires the addition of energy to fuse BT. For this we have to choose negative sign in Eq. (3.14) to ensure positive θ_p. In this paper, we consider the following two cases

Case 1: The fluid in the shell – film and porous – silicon layer is homogeneous and incompressible with temperature, T_p, in the porous – silicon is assumed to be constant which may be higher than fluid temperature.

Case 2: The fluid in the shell – film as well as in porous – silicon is assumed to satisfy Boussinesq approximation with varying temperature T_p and T_f.

Case 1: Homogeneous fluid

$$v_a \frac{\partial \theta}{\partial y} = \frac{1}{R_a} \frac{\partial^2 \theta}{\partial y^2} + N e^{-\Omega_o y} \qquad \textbf{(3.15)}$$

where $R_a = \dfrac{\delta_o h^3}{\kappa_f \mu_f}$ is the Rayleigh number because δ_o has the dimensions of $\rho_o \alpha_T g T_o$, $N = \dfrac{I_o \Omega_o \mu_f}{\delta_o T_o}$ and v_a is given with $\theta_p - \theta_f = \delta(1)$ that is δ *is constant.*

Eqn. (3.15) is solved using the following two set of boundary conditions.

Set 1: $\theta = 1$ *at* $y = 0$, and $\theta = \theta_1$ *at* $y = 1$ **(3.16)**

Set 2: $\theta = 1$ *at* $y = 0$, and $\dfrac{d\theta}{dy} = -B_i (\theta_b - 1)$ *at* $y = 1$ **(3.17)**

Where $B_i = \dfrac{h_c\, h}{\kappa_f}$ is the Biot number, h_c is the heat transfer coefficient from the porous – silicon layer into shell-film, θ_b is the temperature at $y = 1$.

$$\theta(y) = a_o + a_1\, e^{by} - \frac{NR_a e^{-\Omega_o\, y}}{\Omega_o\left(\Omega_o + b\right)} = 1 + \frac{a_o\left(e^{by} - 1\right)}{\left(e^{b} - 1\right)} + a_1\left(1 - e^{-\Omega_o\, y}\right) \qquad \textbf{(3.18)}$$

$$a_o = \theta_1 - 1 - a_1\left(1 - e^{-\Omega_o}\right)\ ,\ \ a_1 = \frac{NR_a}{\Omega_o\left(\Omega_o + b\right)}\ ,\quad b = v_a\, R_a$$

$$-\left(\frac{\partial\theta}{\partial y}\right)_{y=1} = \frac{NR_a}{\left(\Omega_o + b\right)} e^{-\Omega_o} + b\, a_1\, e^{b} \qquad \textbf{(3.19)}$$

Similarly the solution of Eqn. (3.15), satisfying the boundary conditions (3.17), is

$$\theta(y) = 1 + a_2\left(1 - e^{by}\right) + \frac{N R_a \left(1 - e^{-\Omega_o y}\right)}{\Omega_o\left(\Omega_o + b\right)} \qquad \textbf{(3.20)}$$

where

$$\theta_B = a_3\left[1 + \frac{NR_a\left(1 - e^{-\Omega_o}\right)}{\Omega_o\left(\Omega_o + b\right)} + \left(\frac{NR_a e^{-\Omega_o} - \mathrm{B}_i\left(\Omega_o + b\right)}{b\left(\Omega_o + b\right)}\right)\left(e^{-b} - 1\right)\right]$$

$$a_2 = \frac{NR_a e^{-(\Omega_o + b)}}{b(\Omega_o + b)} + \frac{B_i}{b}\left(\theta_B - 1\right)e^{-b}, \qquad a_3 = \frac{1}{\left[1 - \mathrm{B}_i\left(e^{-b} - 1\right)/b\right]}$$

Case 2: Boussinesq fluid

For the shell – film

$$\mathrm{v}_a \frac{\partial \theta_f}{\partial y} = \frac{1}{R_{af}} \frac{\partial^2 \theta_f}{\partial y^2} + N e^{-\Omega_o y} \qquad \textbf{(3.21)}$$

For the porous – silicon layer

$$0 = \frac{\partial^2 \theta_p}{\partial y^2} - N_p e^{-\Omega_o y} \qquad \textbf{(3.22)}$$

where $N_p = \dfrac{I_o \Omega_o h^3}{\kappa_p T_o}$

The boundary conditions on θ_f and θ_p are

$$\frac{\partial \theta_p}{\partial y} \to 0 \qquad \text{as} \qquad y \to \infty, \quad \theta_f = 1 \quad \text{at} \quad y = 0 \qquad \textbf{(3.23)}$$

$$\frac{\partial \theta_f}{\partial y} = -B_i\left(\theta_{f_1} - 1\right), \qquad \frac{\partial \theta_p}{\partial y} = -B_i\left(\theta_{p_1} - 1\right) \quad \text{at} \quad y = 1 \qquad \textbf{(3.24)}$$

θ_{f_1} and θ_{p_1} are the values of θ_f and θ_P at y =1

The solution of Eq. (3.21) and Eq. (3.22) satisfying the above boundary conditions are

$$\theta_f = 1 + a_1\left(1 - e^{-\Omega_o y}\right) + \frac{B_i}{b}\left(\theta_{f_1} - 1\right)e^{-b}\left(1 - e^{b y}\right) + \frac{\Omega_o a_1}{b}\; e^{-(\Omega_o + b)}\left(1 - e^{b y}\right)$$

and

$$\theta_p = 1 + \frac{N_p}{\Omega_o B_i}e^{-\Omega_o} + \frac{N_p}{\Omega_o^2}\left(e^{-\Omega_o} - e^{-\Omega_o y}\right)$$

From these we have

$$\delta(1) = \theta_{p_1} - \theta_{f_1} = 1 - a_3 - \frac{N_p}{\Omega_o B_i}e^{-\Omega_o} - a_3\left[a_1\left(1 - e^{-\Omega_o}\right) + \frac{\left(B_i - \Omega_o a_1 e^{-\Omega_o}\right)}{b}\left(1 - e^{-b}\right)\right]$$

4. CONCLUSIONS

The linear RTI in an IFE target modeled as a thin electrically conducting fluid film in the presence of transverse magnetic field lined with an incompressible electrically conducting fluid saturated nanostructured porous lining with uniform densities is investigated using normal mode analysis. The main objective of this study is to show that the two mechanisms, having a suitable strength of magnetic filed and suitable porous material made up of nanostructure lining, reduce the growth rate of ablative surface of IFE target considerably compared to that in the absence of these two mechanisms. The dispersion relations given by Eqs. (3.3) to (3.7) are analogous to the one given by Takabe *et al.,* (1985) for compressible non-viscous nonelectrically conducting fluid

as shown in Eqn. (1.2). The dispersion relation (3.7) coincides with the one given by Rudraiah (2003) in the absence of Magnetic field. The dispersion relation given by Eqn. (3.6) coincides with the one given by Babchin *et al.,* (1983) in the absence of magnetic field (M$\rightarrow$0) and the nanostructure porous lining ($\sigma \rightarrow 0$).

Setting *n*=0 in Eqn. (3.3), we obtain the cutoff wave number, ℓ_{ct} , above which MRTI mode is stabilized and which is found to be

$$\ell_{ct} = \sqrt{\delta B} \qquad \textbf{(4.1)}$$

For homogeneous fluid δ =1 and for Boussinesq fluid $\sigma = \theta_{p_1} - \theta_{f_1}$. The maximum wave number, ℓ_m, obtained from Eqn. (3.3) by setting $\frac{\partial n}{\partial \ell} = 0$, is

$$\ell_m = \sqrt{\left(\theta_{p_1} - \theta_{f_1}\right)\frac{B}{2}} = \frac{\ell_{ct}}{\sqrt{2}} \qquad \textbf{(4.2)}$$

The results given by Eqs. (4.1) and (4.2) are also true even for the cases in the absence of both nanostructure porous lining and magnetic field. The corresponding maximum growth rates, denoted by suffix *m*, from Eqs. (3.3) to (3.10) are

$$n_m = \frac{B}{4}\left(\frac{1}{3} - \Delta_1\right) \quad \text{or} \quad \frac{B}{4}\left(\frac{1}{3} - \Delta_1\right)\left(\theta_{p_1} - \theta_{f_1}\right)^2 \qquad \textbf{(4.3)}$$

$$n_{1m} = \frac{B}{4}\left(\frac{1}{3} - \frac{\alpha\sigma}{4(1+\alpha\sigma)}\right) \quad \text{or} \quad \frac{B}{4}\left(\frac{1}{3} - \frac{\alpha\sigma}{4(1+\alpha\sigma)}\right)\left(\theta_{p_1} - \theta_{f_1}\right)^2 \qquad \textbf{(4.4)}$$

$$n_{2m} = \frac{B}{4}\left(\frac{1}{3} - \Delta\right) \quad \text{or} \quad \frac{B}{4}\left(\frac{1}{3} - \Delta\right)\left(\theta_{p_1} - \theta_{f_1}\right)^2 \qquad \textbf{(4.5)}$$

$$n_{bm} = \frac{B}{12} \quad \text{or} \quad \frac{B}{12}\left(\theta_{p_1} - \theta_{f_1}\right)^2 \tag{4.6}$$

where

$$\Delta = \frac{M^3 - 3\left(M - thM\right)}{3\,M^3} \tag{4.7}$$

$$\Delta_1 = \frac{M^2 - 3}{3\,M^2} + \frac{M\ th\,M + \dfrac{2\,\alpha\,\sigma\,(ch\,M - 1)}{ch\,M}}{M^3\,(M + \alpha\,\sigma\,th\,M)} \tag{4.8}$$

From these, we get

$$G_{0m} = \frac{n_m}{n_{bm}} = 1 - 3\,\Delta_1 \tag{4.9}$$

$$G_{1m} = \frac{n_{1m}}{n_{bm}} = \frac{\left(4 + \alpha\sigma\right)}{4\left(1 + \alpha\sigma\right)} \tag{4.10}$$

$$G_{2m} = \frac{n_{2m}}{n_{bm}} = \frac{3\left(M - \tanh M\right)}{M^3} \qquad \textbf{(4.11)}$$

$$G_{3m} = \frac{n_m}{n_{1m}} = \frac{4\left(1 - 3\Delta_1\right)\left(1 + \alpha\sigma\right)}{\left(4 + \alpha\sigma\right)} \qquad \textbf{(4.12)}$$

$$G_{4m} = \frac{n_m}{n_{2m}} = \frac{\left(1 - 3\Delta_1\right)}{\left(1 - 3\Delta\right)} \qquad \textbf{(4.13)}$$

$$G_{5m} = \frac{n_{3m}}{\left(n_b\right)_{pm}} = \frac{12\left(1 + \alpha\sigma\right)}{\left(4 + \alpha\sigma\right)} \left[\frac{M + \left(\alpha\sigma - 1\right) thM + \dfrac{2\alpha\sigma\left(1 - ChM\right)}{M\ ChM}}{M^3\left(1 + \alpha\sigma\ \dfrac{thM}{M}\right)} \right] \qquad \textbf{(4.14)}$$

It will be of interest to compare these results with those given in Eqn. (1.2) by Takabe *et al*., (1985) for compressible fluid. In their case

$$\left(\ell_{ct}\right)_{Ta} = \frac{0.81g}{\beta^2 \mathrm{v}_a^2} \quad \text{and} \quad \left(\ell_m\right)_{Ta} = \frac{0.81g}{4\beta^2 \mathrm{v}_a^2} = \frac{\left(\ell_{ct}\right)_{Ta}}{4} \qquad \textbf{(4.15)}$$

The corresponding n_m is

$$\left(n_m\right)_{T_a} = 0.45\sqrt{\left(\ell_m\right)_{T_a} g} = 0.45\left(n_b\right)_{T_a} \qquad \textbf{(4.16)}$$

$$\left(n_b\right)_{T_a} = \sqrt{\left(\ell_m\right)_{T_a} g} \qquad \textbf{(4.17)}$$

and the quantities with suffix T_a correspond to those given by Takabe *et al*., (1985).

Using Eqn. (4.15) Takabe et.al. (1985) have shown that the maximum growth rate was reduced to 45% of their classical result given by Eqn. (4.16).

From Eqn. (4.8), Rudraiah, (2003) has shown that in the absence of magnetic field and in the presence of porous lining, the reduction of maximum growth rate depends on the characteristics α and σ of porous lining. For the types of porous material, namely, foametal, α takes the value 0.1 and σ ranges from 4 to 20 and for aloxite materials α = 4 and σ ranges from 4 to 20 (see the experiments of Beavers and Joseph (1967). Then for α =0.1 and σ =4 Rudraiah (2003) has shown that the maximum growth rate given by Eqn. (4.8) has been reduced to 78.57% of the classical value given by Eqn. (4.6). In the presence of magnetic field and absence of porous lining it is clear that the maximum growth rate given by Eqn. (4.9) depends on the Hartman number *M*. We note that the ratio depends purely on nanostructured porous lining when *M*=0, the ratio given by Eqn. (4.8) will depend only on the values of *M* in the absence of porous lining where as other ratios depend on *M, α* and *σ*.

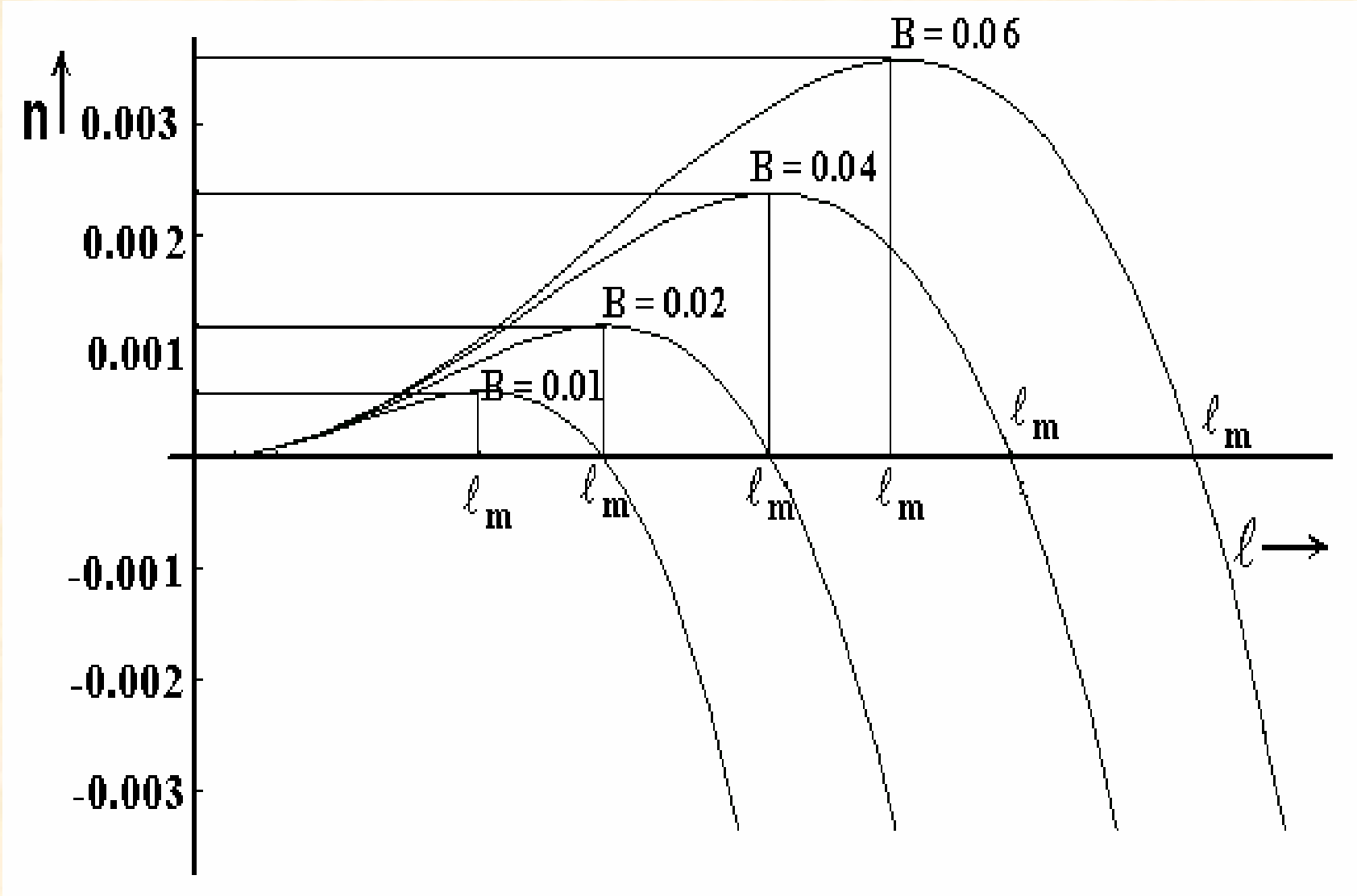

Fig 2: The Growth Rate *n* versus wave number for *M* =1 and for different Bond numbers *B*

The relation (3.3) is plotted in Fig.2 which is for the growth rate *n* versus the wave number ℓ for *M*=1, $\alpha = 0.1$, and σ = 4 for different values of *B*. From this fig.2 we conclude that the perturbation of the interface having a wave number smaller than ℓ_{ct} are amplified when $\delta > 0\ (i.e., \rho_f < \rho_p)$ and the growth rate decreases with a decrease in B implying increase in surface tension. That is, increase in surface tension makes the interface more stable even in the case of electrically conducting fluid. Similar behavior is observed for *M*>1 for fixed values of α and σ and found that increase in σ is more significant than an increase in M in reducing the growth rate.

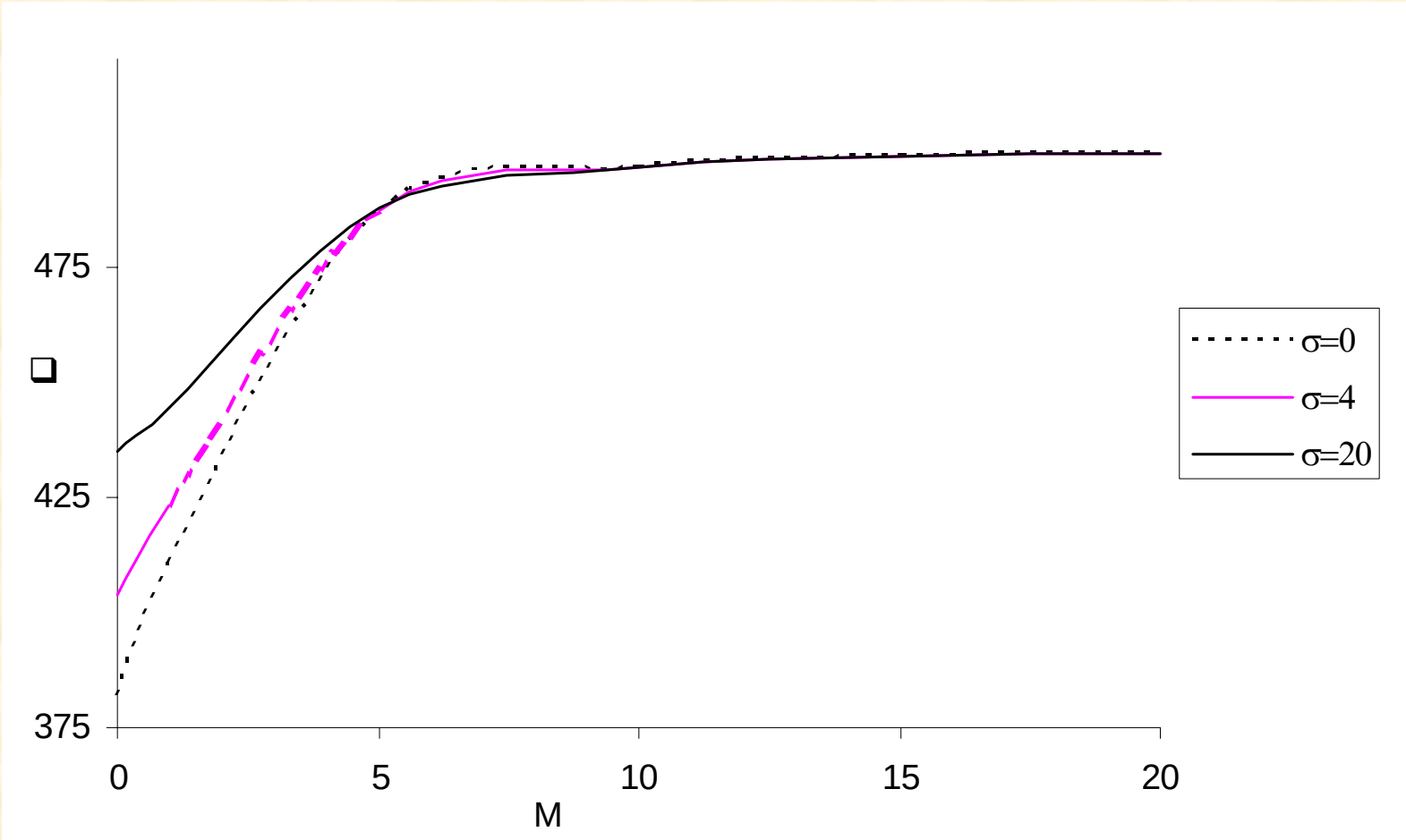

Fig 3. Ablative surface Temperature θ_b for different ♦

Table 4: The values of θ_b

♦	M=0	M=1	M=10	M=20
0	382.264	410.918	496.739	498.861
4	403.504	423.383	496.756	498.865
8	416.156	431.443	496.772	498.868
12	424.549	437.081	496.786	498.871
16	430.523	441.247	496.799	498.874
20	434.991	444.45	496.812	498.876

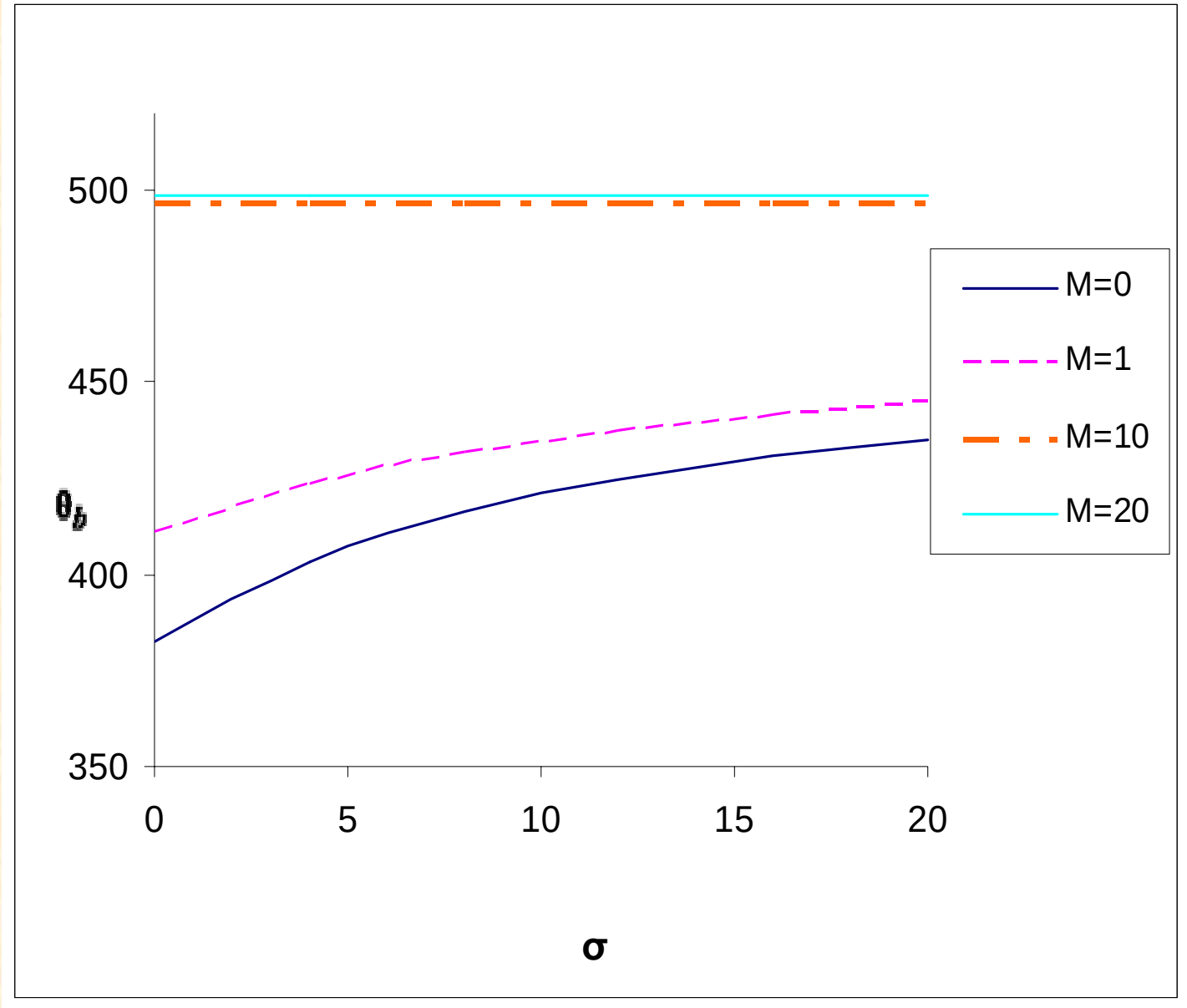

Fig 4. Ablative surface Temperature θ_b for different M.

Table 5: The values of θ_b

M	♦	♦	♦
0	382.3	403.5	434.99
1	410.9	423.4	444.5
5	486.9	487.1	487.5
10	496.7	496.8	496.8
15	498.86	498.86	498.88
20	499.64	499.64	499.65

The ablative temperature θ_B given by equation (3.20) is computed for different values of *M* and σ. The results of θ_B vs *M* for different values of σ are plotted in fig. 3 and θ_B vs σ for different values of *M* are drawn in fig. 4. From these figures, we conclude that for small values of *M* and σ, θ_B increases slowly and saturates for larger values of *M* and σ

Acknowledgement:

This work is supported by IAEA, Vienna under IFE-CRP project No. IND 11534. Its financial support is gratefully acknowledged.

References:

1. Babchin, A. J. Frenkel, A. L., Levich, B. G., Shivashinske, G.I., (1983), Phys., Fluids, 26, pp 3159.

2. Betti, R., Goncharov, V.N., McGroy, R.L. and Verdon, C. P., (1995), Phys., Plasmas 2, pp 3844.

3. Kilkenny, J.D., Glendinning, S.G., Hann, S.W., Hamurel, B.A., Lindl, J.D., Munro, B.A., Remington, S.V., Weber, J.P., Kanauer, J.P. and Verdon, C.P., (1994), Phys., Plasma 1, pp 379.

4. Knauer, J.P. et al (2002), Phys., Fluids, 7(1), pp 338.

5. Lindl, J.D. (1995), Phys., Plasma 2, pp 3933.

6. Rudraiah, N. (2003), Fusion Sci. and Tech., 43, pp 307

I. KHI at the ablative surface lined with nano structured porous layer in a fully developed two-phase composite layer using BJR condition.

In the third year of the project, in contribution 4, we have considered KHI in a sparsely packed porous lining, where the Brinkman equation is valid and the interface between the film and the porous lining is assumed to be a regular surface and using Residual shear condition. In these problems the thickness of the porous layer was absent. In many practical applications including IFE, it is important to find the effect of the thickness of porous lining. This can be done using Rudraiah (1985) boundary condition. As the thickness becomes very large Rudraiah condition tends to Beavers-Joseph (BJ - 1967) condition. Hence in the literature Rudraiah condition is denoted by BJR condition. In the first quarter of the fourth year of the project, we propose to investiage RTI in a finite thickness of porous layer using BJR condition with the objective of predicting the effect of the thickness of porous lining on the reduction of growth rate of KHI. This effect is important in the design of effective IFE target.

II. Kelvin-Helmholtz Instability at the ablative surface using external constraints of magnetic field and porous lining.

In the remaining quarters of the fourth year of the project, we propose to investigate the effect of magnetic field on the reduction of growth rate using the following cases:

Case 1: Effects of densely packed porous lining in the presence of a magnetic field on KHI growth rate using BJ condition.

Case 2: Effects of sparsely packed porous layer in the presence of magnetic field on the KHI growth rate using residual shear condition.

Case 3: Effects of sparsely packed finite thickness porous lining in the presence of a magnetic field on the KHI growth rate using BJR condition. This condition predicts the effect of thickness of porous lining.

Case 4: Effects of magnetic field and roughness of the ablative surface on the reduction of KHI growth rate. The results obtained in this case will be useful to take care of the roughness of the IFE design.

The problem 2 posed above involves four cases and each case take considerable time because we have to solve plasma equations in thin film and porous lining using normal mode analysis, Kinematics condition in the presence of surface tension and dynamic condition.

In first quarter of fourth year we proposed to investigate the problem 1 posed above and in the remaining three quarters we propose to investigate cases 1 and 4 posed in problem 2 above.

If time permits, we initiate the third type of instability, namely Richtmyer and Meskov instability proposed in our section on "Objectives". This instability is also important in the design of IFE target. Here also, we propose to study the effects of nano structure porous lining and the external magnetic field using cases 1 to 4 proposed in problem 2 above.

Table 2(a):Values of G^{mi} for different values of M and σ =4, α =0.1

M	G_{mo}	G_{m1}	G_{m2}	G_{m3}	G_{m4}	G_{m5}
0.5	0.7296	0.7857	0.9092	0.9286	0.8025	0.9286
1.0	0.6013	0.7857	0.7152	0.7653	0.8407	0.7653
1.5	0.4657	0.7857	0.5288	0.5926	0.8806	0.5926
2.0	0.3546	0.7857	0.3885	0.4513	0.9128	0.4513
2.5	0.272	0.7857	0.2906	0.3462	0.9360	0.3462
3.0	0.2122	0.7857	0.2228	0.2700	0.9524	0.2700
3.5	0.1687	0.7857	0.1751	0.2143	0.9638	0.2147
4.0	0.1367	0.7857	0.1407	0.1740	0.9719	0.1740
4.5	0.1127	0.7857	0.1152	0.1434	0.9777	0.1434
5.0	0.0943	0.7857	0.0960	0.1120	0.9820	0.1198
5.5	0.0799	0.7857	0.0811	0.1017	0.9852	0.1017
6.0	0.0686	0.7857	0.0694	0.0873	0.9876	0.0873

Table 2(b): Values of G_{mi} for different values of M and σ =10, α =0.1

M	G_{mo}	G_{m1}	G_{m2}	G_{m3}	G_{m4}	G_{m5}
0.5	0.5896	0.6250	0.9092	0.9434	0.6485	0.9434
1.0	0.5043	0.6250	0.7100	0.8000	0.7000	0.8068
1.5	0.4066	0.6250	0.5288	0.6506	0.7689	0.6506
2.0	0.3203	0.6250	0.3900	0.5100	0.8200	0.5125
2.5	0.2520	0.6250	0.2906	0.4032	0.8673	0.4032
3.0	0.2002	0.6250	0.2200	0.3200	0.8900	0.3203
3.5	0.1613	0.6250	0.1751	0.2581	0.9215	0.2581
4.0	0.1320	0.6250	0.1400	0.2100	0.9300	0.2111
4.5	0.1095	0.6250	0.1152	0.1752	0.9503	0.1752
5.0	0.0920	0.6250	0.0960	0.1470	0.9600	0.1474
5.5	0.0784	0.6250	0.0811	0.1255	0.9664	0.1255
6.0	0.0670	0.6250	0.0690	0.1070	0.9710	0.1080

Table 2(c): Values of G_{mi} for different values of M and σ =20, α =0.1

M	G_{mo}	G_{m1}	G_{m2}	G_{m3}	G_{m4}	G_{m5}
0.5	0.4775	0.5000	0.9090	0.9550	0.5250	0.9549
1.0	0.4210	0.5000	0.7150	0.8410	0.5880	0.8413
1.5	0.3510	0.5000	0.5290	0.7030	0.6640	0.7025
2.0	0.2860	0.5000	0.3880	0.5710	0.7350	0.5711
2.5	0.2300	0.5000	0.2910	0.4610	0.7930	0.4609
3.0	0.1870	0.5000	0.2230	0.3730	0.8380	0.3733
3.5	0.1530	0.5000	0.1750	0.3050	0.8720	0.3051
4.0	0.1260	0.5000	0.1410	0.2520	0.8970	0.2523
4.5	0.1060	0.5000	0.1150	0.2110	0.9160	0.2111
5.0	0.0890	0.5000	0.0960	0.1790	0.9300	0.1787
5.5	0.0760	0.5000	0.0810	0.1530	0.9420	0.1528
6.0	0.0660	0.5000	0.0690	0.1320	0.9500	0.1320

Table 3(a): Values of G_{mi} for different values of M and σ =4, α =4

M	G_{mo}	G_{m1}	G_{m2}	G_{m3}	G_{m4}	G_{m5}
0.5	0.2860	0.2941	0.9092	0.9726	0.3146	0.9725
1.0	0.2643	0.2941	0.7152	0.8986	0.3695	0.8986
1.5	0.2346	0.2941	0.5288	0.7978	0.4438	0.7978
2.0	0.2029	0.2941	0.3885	0.6898	0.5222	0.6898
2.5	0.1729	0.2941	0.2906	0.5878	0.5950	0.5878
3.0	0.1466	0.2941	0.2228	0.4983	0.6579	0.4983
3.5	0.1243	0.2941	0.1751	0.4226	0.7100	0.4226
4.0	0.1058	0.2941	0.1407	0.3598	0.7524	0.3598
4.5	0.0907	0.2941	0.1152	0.3083	0.7868	0.3082
5.0	0.0782	0.2941	0.0960	0.2659	0.8146	0.2659
5.5	0.0679	0.2941	0.0811	0.2310	0.8373	0.2310
6.0	0.0594	0.2941	0.0694	0.2021	0.8560	0.2021

Table 3(b): Values of G_{mi} for different values of M and σ =10, α =4

M	G_{mo}	G_{m1}	G_{m2}	G_{m3}	G_{m4}	G_{m5}
0.5	0.2614	0.2683	0.9092	0.9744	0.2875	0.9744
1.0	0.2428	0.2683	0.7152	0.9050	0.3395	0.9050
1.5	0.2171	0.2683	0.5288	0.8092	0.4106	0.8092
2.0	0.1891	0.2683	0.3885	0.7050	0.4869	0.7050
2.5	0.1624	0.2683	0.2906	0.6052	0.5588	0.6052
3.0	0.1385	0.2683	0.2228	0.5164	0.6219	0.5164
3.5	0.1182	0.2683	0.1751	0.4404	0.6749	0.4404
4.0	0.1011	0.2683	0.1407	0.3768	0.7187	0.3767
4.5	0.0869	0.2683	0.1152	0.3240	0.7444	0.3240
5.0	0.0752	0.2683	0.0960	0.2804	0.7837	0.2804
5.5	0.0656	0.2683	0.0811	0.2443	0.8078	0.2443
6.0	0.0575	0.2683	0.0694	0.2143	0.8278	0.2143

Table 3(c): Values of G_{mi} for different values of M and σ =20, α =4

M	G_{mo}	G_{m1}	G_{m2}	G_{m3}	G_{m4}	G_{m5}
0.5	0.2528	0.2593	0.9092	0.9750	0.2780	0.9750
1.0	0.2352	0.2593	0.7152	0.9071	0.3288	0.9071
1.5	0.2108	0.2593	0.5288	0.8130	0.3986	0.8130
2.0	0.1841	0.2593	0.3885	0.7101	0.4739	0.7101
2.5	0.1584	0.2593	0.2906	0.6111	0.5453	0.6111
3.0	0.1355	0.2593	0.2228	0.5226	0.6082	0.5223
3.5	0.1158	0.2593	0.1751	0.4465	0.6613	0.4465
4.0	0.0992	0.2593	0.1407	0.3862	0.7052	0.3826
4.5	0.0854	0.2593	0.1152	0.3295	0.7413	0.3295
5.0	0.0740	0.2593	0.0960	0.2855	0.7710	0.2855
5.5	0.0646	0.2593	0.0811	0.2490	0.7955	0.2490
6.0	0.0567	0.2593	0.0694	0.2185	0.8158	0.2185

Thank you